Performance Evaluation of Wavelet De-Noising Schemes for Suppression of Power Line Noise in Electrocardiogram Signals

Y. K. Ahmed[1*], A. R. Zubair[2]

[1]Department of Biomedical Engineering, University of Ilorin, Ilorin, Nigeria.
[2]Department of Electrical and Electronic Engineering, University of Ibadan, Ibadan, Nigeria.

ABSTRACT: Power line noise introduces distortions to recorded electrocardiogram (ECG) signals. These distortions compromise the integrity and negatively affect the interpretation of the ECG signals. Despite the fact that the amplifiers used in biomedical signal processing have high common mode rejection ratio (CMRR), ECG recordings are still often corrupted with residual Power Line Interference (PLI) noise. Further improvement in the hardware solutions do not have significant achievements in PLI noise suppression but rather introduce other adverse effects. Software approach is necessary to refine ECG data. Evaluation of PLI noise suppression in ECG signal in the wavelet domain is presented. The performance of the Hard Threshold Shrinkage Function (HTSF), the Soft Threshold Shrinkage Function (STSF), the Hyperbola Threshold Shrinkage Function (HYTSF), the Garrote Threshold Shrinkage Function (GTSF), and the Modified Garrote Threshold Shrinkage Function (MGTSF) for the suppression of PLI noise are evaluated and compared with the aid of an algorithm. The optimum tuning constant for the Modified Garrote Threshold Shrinkage Function (MGTSF) is found to be 1.18 for PLI noise. GTSF is found to have best performance closely followed by MGTSF in term of filtering Gain. HTSF recorded the lowest Gain. Filtering against PLI noise in the wavelet domain preserves the key features of the signal such as the QRS complex.

KEYWORDS: Electrocardiogram, power line noise, biomedical amplifier, wavelet transformation, wavelet threshold, shrinkage functions.

[Received Nov. 9, 2020; Revised May 4, 2021; Accepted May 15, 2021] Print ISSN: 0189-9546 | Online ISSN: 2437-2110

I. INTRODUCTION

Bio-electric signals have been very useful in diagnostics and physiological monitoring applications (McSharry et al., 2003; Opie, 2004). Electrocardiogram (ECG) is among the most utilised bio-signals as it is a representation of the electrical activity of the heart in graphical form (Castillo et al., 2013). This activity depicts the action potential, invoked by muscular contraction and relaxation of the heart which varies with prevailing health condition (Dandapat et al., 2015). This information is useful for the detection of various types of heart disorder (Dandapat et al., 2015).

The ECG signal has important diagnostic features marked with hills and valleys as shown in Figure 1. These features are the P-wave, QRS-complex, T-wave, and U-wave. The QRS-complex indicates ventricular contraction while T-wave indicates ventricular relaxation. The U-wave, though not common, indicates delayed purkinje fibres depolarization (Opie, 2004; Dandapat et al., 2015).

The ECG signal S(n) may be corrupted with noise signals η(n) during acquisition as electrodes are conventionally attached to the human skin to pick the signals (Romero et al., 2012; Akwei-Sekyere, 2015; Zubair et al., 2018). This is illustrated in Eqn. (1) and Figure 2 (Zubair et al., 2018). The noise signals include PLI noise introduced by a 50/60Hz AC mains supply, the baseline wander noise generated by lead placement on bone, the rhythmic movement of the chest while breathing and restless movement, and the Electromyography (EMG) noise on the other hand is introduced by the high frequency muscle activities (Zubair et al., 2018; Aqil et al., 2017; Ravandale and Jian, 2015).

$$X(n) = S(n) + \beta\eta(n) \quad (1)$$

where $X(n)$ is the corrupted signal; β is the noise amplification factor.

The PLI noise or simply Power line noise is a significant artefact in the ECG signal. PLI has a band width of less than 1 Hz; It is a narrow-band noise centred at the mains supply frequency of 50Hz or 60Hz (Castillo et al., 2013). Hence, PLI interferes with the ECG signal which has a frequency range of 0.5 Hz – 150 Hz (Aqil et al., 2017). Power line noise introduces distortions to recorded ECG signals. These distortions compromise the integrity and negatively affect the interpretation of the ECG signals (Akwei-Sekyere, 2015). Suppression of Power line noise is necessary in bioengineering, neural engineering, neurosurgery, cardiology and drug discovery (Akwei-Sekyere, 2015).

*Corresponding author: ahmed.yk@unilorin.edu.ng
doi: http://dx.doi.org/10.4314/njtd.v18i2.9

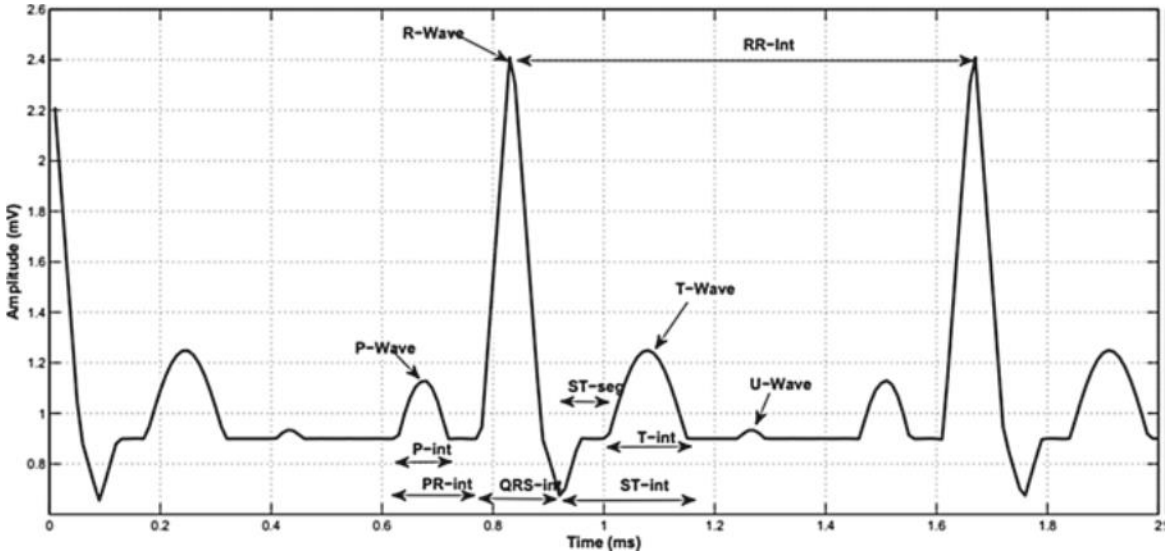

Figure 1: Typical ECG signal waveform (McSharry et al., 2003).

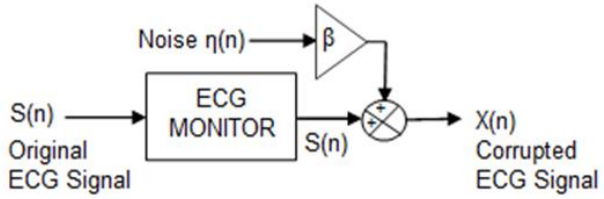

Figure 2: Dynamics of ECG Signal Corruption with noise (Zubair et al., 2018).

Many approaches have been developed for PLI suppression in ECG signals. The hardware approaches include the use of biomedical amplifiers with amplified CMRR. Despite high CMRR, ECG data are diffused with residual power-line interference due to differences in the electrode impedances. Hence, a false differential signal is created such that an infinitely high CMRR cannot suppress (Chavdar et al., 2005). PLI interferes with the correct boundaries and features of the ECG leading to inaccurate ECG analysis and diagnosis (Chavdar et al., 2005). Further improvement in the hardware solutions do not have significant achievements in PLI noise suppression but rather introduce other adverse effects (Chavdar et al., 2005; Lin and Hu, 2007); Hence, the need for the introduction of software based signal processing solutions (Chavdar et al., 2005). Notable among these software approaches are the window filtering methods such as the rectangular window filtering method which are computationally easy but suboptimal (El Bouny et al., 2019; Alfaouri and Daqrouq, 2008) and the subtraction procedure.

Empirical Mode Decomposition (EMD), being a data driven technique was implemented by Suchetha et al. (2017) to filter 50Hz noise from ECG signal; however, EMD is not robust to small perturbation (Aqil et al., 2017). Numerous adaptive filtering techniques such as the Least Mean Square (LMS), normalized LMS and Recursive Least Square (RLS) among others have been used by Romero et al. (2012) in suppressing PLI noise from ECG signal. Dwivedi et al. (2020) used ensemble approach in ECG noise reduction. Although, ensemble approach yielded a good result, it was computationally complex. Statistical approach such as the Independent Component Analysis (ICA) has also been used by (Akwei-Sekyere, 2015). Genetic algorithms and artificial intelligence technique have also been applied to ECG noise removal (Mateo et al., 2008). In recent time, wavelet transform technique has been increasingly explored in PLI noise suppression with good results (Chmelka, 2005). Wavelet technique preserves the ECG morphological features which are essential for accurate diagnosis (Tiwari and Dubey, 2014; Huimin et al., 2012). El-Bouny et al. (2017) used undecimated wavelet transform to remove PLI noise from ECG signal while Castillo et al. (2013) used a one–step wavelet processing technique to reduce artefacts in ECG signal. Stationary wavelet transform coupled with interval threshold technique was proposed by (El-Bouny et al., 2017; El-Bouny et al., 2018) to reduce ECG affiliated noise.

In this work, suppression of PLI noise in wavelet domain was studied with the help of an algorithm developed in MATLAB working environment. The performance of the Hard Threshold Shrinkage Function (HTSF), the Soft Threshold Shrinkage Function (STSF), the Hyperbola Threshold Shrinkage Function (HYTSF), the Garrote Threshold Shrinkage Function (GTSF), and the Modified Garrote Threshold Shrinkage Function (MGTSF) for the suppression of PLI noise are evaluated and compared.

II. THEORETICAL BACKGROUND

A. Materials

Signal transformation is usually done to simplify signal processing. The Fourier transform, being a very popular transform can only present the frequency components of a signal that is stationary (Zubair and Ahmed, 2019; El Bouny et al., 2018; Aqil et al., 2015; Goswami and Chan, 2011). However, physiological signals are non-stationary and can best be processed in wavelet transform (Goldberger et al., 2000). Wavelet transform can present the non-stationary signals simultaneously in time and frequency domains and is widely adopted in signal noise suppression or compression tasks (Zubair, 2019).

The energy of a small wave (wavelet) is concentrated in time (Zubair and Ahmed, 2019). Wavelet families include Coiflets, Spline, Haar, Daubechies (Db) among others. Figure 3 illustrated the wavelet decomposition of a corrupted signal in to two parts with L levels. Part A is the approximate coefficients containing the low-frequency information of the signal while part D is the details components of the coefficients and it contains information about the high-frequency part of the signal. Low pass (lp) and high pass (hp) filters are used to generate A and D respectively. Given that Y is the wavelet transform of X. The approximate component Ya(n) of Y and Detail component Yd(n) of Y are related to A and D as indicated in Figure 3 (Zubair et al., 2018; Van Fleet, 2011; Donoho and Johnstone, 1994).

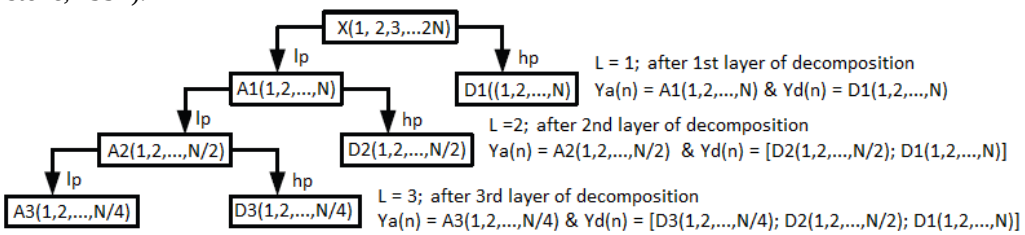

Figure 3: A three level wavelet decomposition diagram.

B. Wavelet Shrinkage Function Schemes

The overall block diagram of the noise suppression process of wavelet transform using threshold shrinkage function is shown in Figure 4. The input to the scheme is a 1 by 2N sequence corrupted ECG signal X. Discrete Wavelet decomposition (DWT) at level L, transforms X to a 1 by 2N sequence, Y (Zubair and Ahmed, 2019; Van Fleet, 2011; Donoho and Johnstone, 1994). This Y is sorted into Approximation coefficients Ya and Detail Coefficients Yd. while Yd is modified and shrank by relevant functions to become Ydm, Ya is preserved. In the end, Ya and Ydm are recombined to yield the wavelet transformed coefficients, Yf. Using the Inverse Discrete Wavelet Transform at level L, Yf is inverse-transformed to Xf (Zubair and Ahmed, 2019; Van Fleet, 2011; Donoho and Johnstone, 1994). The recovered signal after the filtering process, Xf is expected to be similar in structure and content to the original ECG signal S of Figure 2. Features such as the QRS complex and R-R interval are preserved by this scheme.

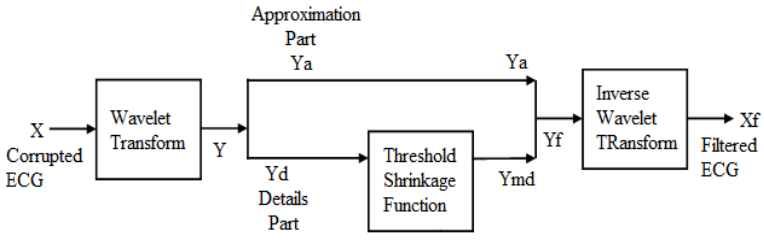

Figure 4: ECG Wavelet threshold shrinkage function de-noising scheme.

In order to achieve noise suppression, a Threshold Shrinkage Function is used to modify the detail part Yd to give modified detail part Ymd. Any element in Yd which is equal to or less than a threshold is set to zero while an element which is greater than the threshold is modified.

The Threshold Shrinkage functions considered in this work are the HTSF, STSF, HYTSF, GTSF and MGTSF which are defined by Eqns. (2), (3), (4), (5), and (6) respectively (Zubair et al., 2018; Van Fleet, 2011). σ, t and λ are defined as the noise level, universal threshold and modified universal threshold respectively and are given by Eqns. (7), (8), and (9) respectively (Zubair and Ahmed, 2019; Van Fleet, 2011; Donoho and Johnstone, 1994;). To achieve noise suppression, the universal threshold t proposed by Donoho and Johnstone (1994) also called Visu shrink is adopted. A modified universal threshold λ which is a product of the universal threshold t and a tuning constant (α) as shown in Eqn. (9) is used for the Modified Garrote Threshold Shrinkage Function (MGTSF).

$$Y_{md}(i,j) = \begin{cases} Y_d(i,j) & \text{for } |Y_d(i,j)| > t \\ 0 & \text{otherwise} \end{cases} \quad (2)$$

$$Y_{md}(i,j) = \begin{cases} \text{sgn}[Y_d(i,j)](|Y_d(i,j)| - t) & \text{for } |Y_d(i,j)| > t \\ 0 & \text{otherwise} \end{cases} \quad (3)$$

$$Y_{md}(i,j) = \begin{cases} \text{sgn}[Y_d(i,j]\sqrt{([Y_d(i,j)]^2 - t^2)} & \text{for } |Y_d(i,j)| > t \\ 0 & \text{otherwise} \end{cases} \quad (4)$$

$$Y_{md}(i,j) = \begin{cases} Y_d(i,j) - \dfrac{t^2}{Y_d(i,j)} & \text{for } |Y_d(i,j)| > t \\ 0 & \text{otherwise} \end{cases} \quad (5)$$

$$Y_{md}(i,j) = \begin{cases} \dfrac{[Y_d(i,j)]^2 - (\lambda - \sigma)^2}{Y_d(i,j)} & \text{for } |Y_d(i,j)| > \lambda \\ 0 & \text{otherwise} \end{cases} \quad (6)$$

$$\sigma = \frac{median\,[Y_d]}{0.6745} \quad (7)$$

$$t = \sigma\sqrt{2Log_e(N)} \quad (8)$$

where N is the number of elements in Yd.

$$\lambda = \alpha t \quad (9)$$

This wavelet de-noising scheme performance is evaluated using the Signal to Noise Ratio (SNR) (Kabir and Shahnaz, 2012; Dandapat et al., 2015). SNRc of Eqn. (10) compares the noisy signal X with the original signal S. PSNRf of Eqn. (11) compares the de-noised signal Xf with the original signal S. The Gain of Eqn. (12) is positive if there is some degree of noise suppression.

$$SNR_c = 10log_{10}\frac{\sum_{n=1}^{n=2N}[S(n)]^2}{\sum_{n=1}^{n=2N}[S(n)-X(n)]^2} \quad (10)$$

$$SNR_f = 10log_{10}\frac{\sum_{n=1}^{n=2N}[S(n)]^2}{\sum_{n=1}^{n=2N}[S(n)-Xf(n)]^2} \quad (11)$$

$$Gain = SNR_f - SNR_c \quad (12)$$

Figure 4 is coded into an algorithm in MATLAB working environment using relevant MATLAB resources (MathWorks,

2019). η is the PLI noise; The noise amplification factor, β = 30 is used to simulate noticeable mix of the noise with the test signals. The algorithm is summarised in Table 1 below.

Table 1: PLI noise suppression algorithm.

Step
Initialize ECG signal S by extraction from MIT-BIH Arrhythmia database.
Add 50Hz PLI noise to the ECG signal to obtain the corrupted ECG signal X.
Set the level of wavelet decomposition (L=3) and compute Y [Ya:Yd], the wavelet transform of X.
Obtain the noise level, universal threshold and modified universal threshold
Apply a Wavelet Threshold Shrinkage Function to modify Yd to Ymd.
Obtain Yf [Ya:Ymd] and apply the inverse DWT to reconstruct filtered ECG signal Xf.
Initialize ECG signal S by extraction from MIT-BIH Arrhythmia database.
Compute $PSNR_c$, $PSNR_f$ and the Gain.

III. RESULTS AND DISCUSSION

A. *Test Signals*

Six ECG signals data were obtained from the MIT-BIH Arrhythmia database. The database has recordings of 48 real ECG data obtained from two leads, sampled at 360 Hz for 30 min duration at 11 bit resolution. ECG signals with data record no: 100.dat, 101.dat, 102.dat, 103.dat, 104.dat, and 105.dat were selected. The first 1000 samples of the data were considered for the analysis (Moody and Mark, 2001; Physiobank, 2018). A is the actual amplitude of the ECG signal and An is the normalised amplitude of the signal. A and An are related as described by Eqns. (13) and (14).

$$A = \frac{(A_n - 200)}{2^{10}} \quad (13)$$

$$A_n = (2^{10})A + 200 \quad (14)$$

B. *Tuning constant for the Modified Garrote Threshold Shrinkage Function*

To obtain the optimal tuning constant, the algorithm was tested with the six test ECG signals using the Modified Garrote Threshold Shrinkage Function (MGTSF) for different values of tuning constant α. The outcomes are summarised in Figure 5. The average Gain values obtained for the six test ECG signals for each value of the tuning constant are plotted in Figure 6. In Figure 6, the optimum tuning constant with highest average Gain is 1.18 dB.

C. *Wavelet Threshold Shrinkage Functions*

The algorithm was tested with the six test ECG signals for the other four wavelet Shrinkage Functions namely HTSF, STSF, HYTSF and the GTSF. The results are combined with those obtained for the MGTSF at optimum tuning constant (α=1.18) as presented in Figure 7.

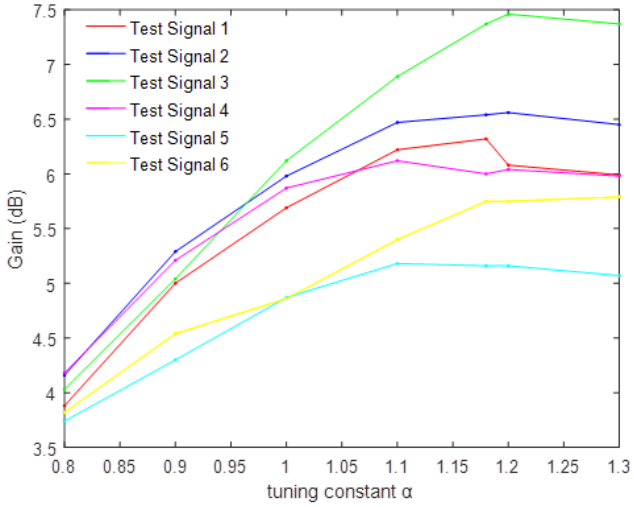

Figure 5: Plots of the gain against the tuning constant for the six test ECG signals with MGTSF.

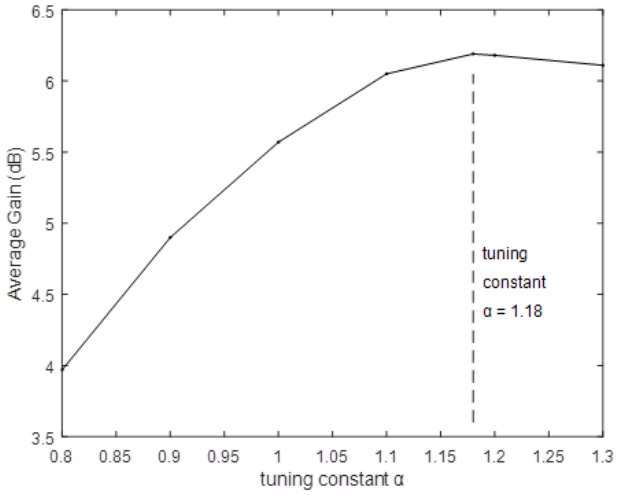

Figure 6: Plots of the average gain for the six test signals against the tuning constant.

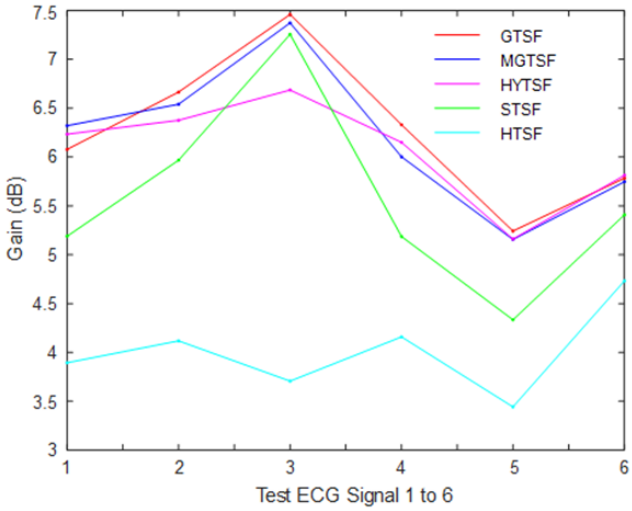

Figure 7: Gain obtained for five wavelet threshold shrinkage functions for the six ECG test signals.

The values of the average Gain obtained by each of the five Threshold Shrinkage Functions are plotted in the bar chart of Figure 8. It shows that GTSF has the best performance closely followed by MGTSF. HTSF recorded the lowest Gain and Average Gain.

The results in term of the waveforms, SNR_c, SNR_f, and the Gain for the five wavelet Threshold Shrinkage Functions for Test ECG Signal 2 are presented in Figure 9 which illustrates the same trend as in Figure 8. For the test ECG signal 1, the MGTSF has a slightly higher Gain than the GTSF as shown in Figure 10. The GTSF results in term of the waveforms, SNR_c, SNR_f, and the Gain for the test ECG Signals 3 to 6 are presented in Figs. 11 and 12. Observation of the filtered ECG waveforms shows the preservation of the important features of the ECG signal such as the R-R wave peaks and QRS complex.

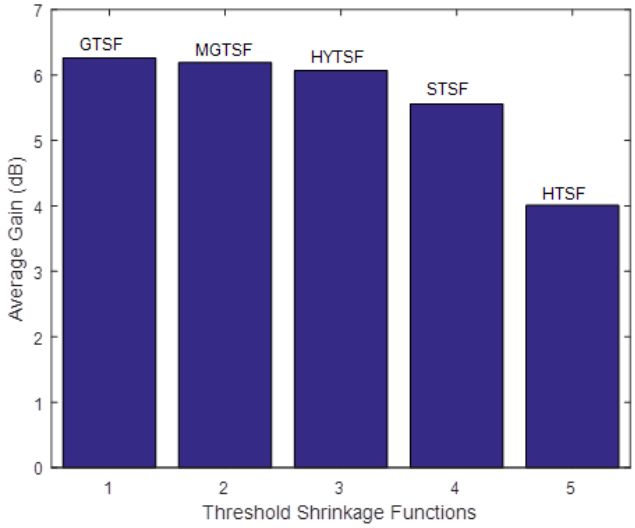

Figure 8: Average gain obtained for five wavelet threshold shrinkage functions.

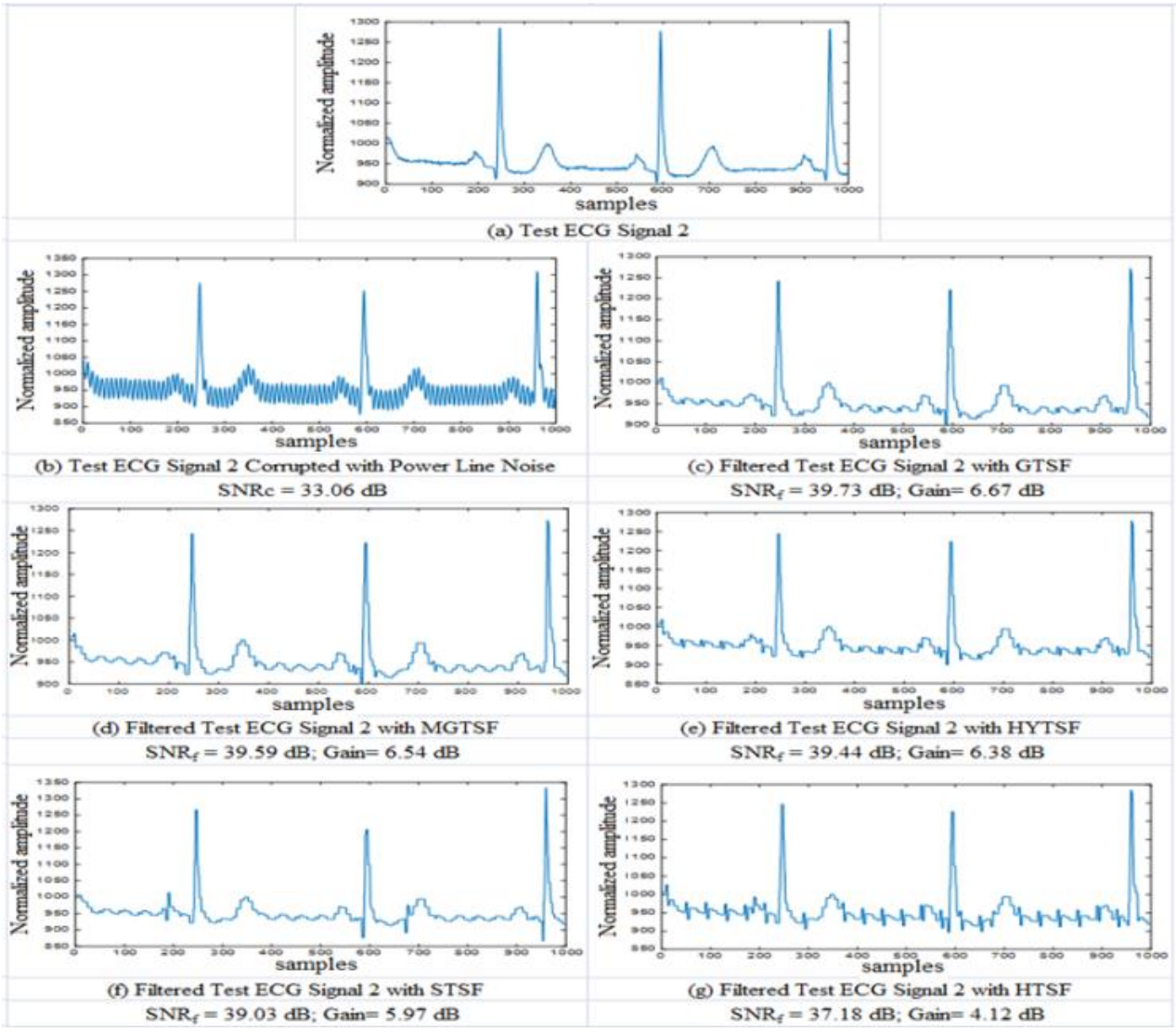

Figure 9: GTSF, MGTSF, HYTSF, STSF and HTSF results for the test ECG signal 2.

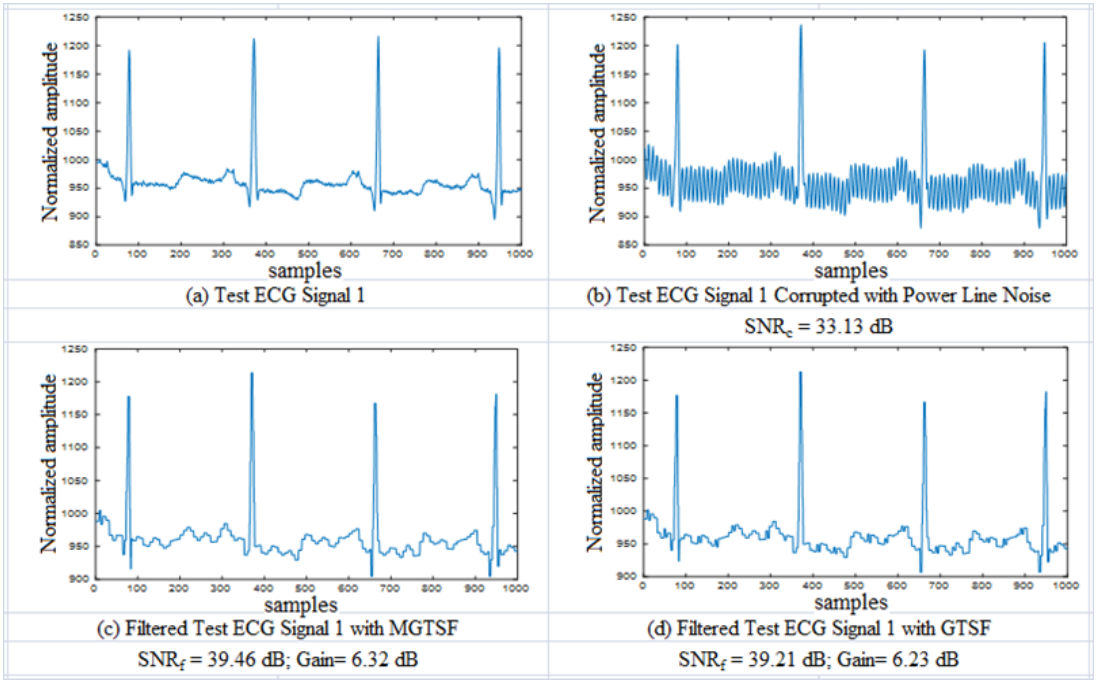

Figure 10: GTSF and MGTSF results for the test ECG signal 1.

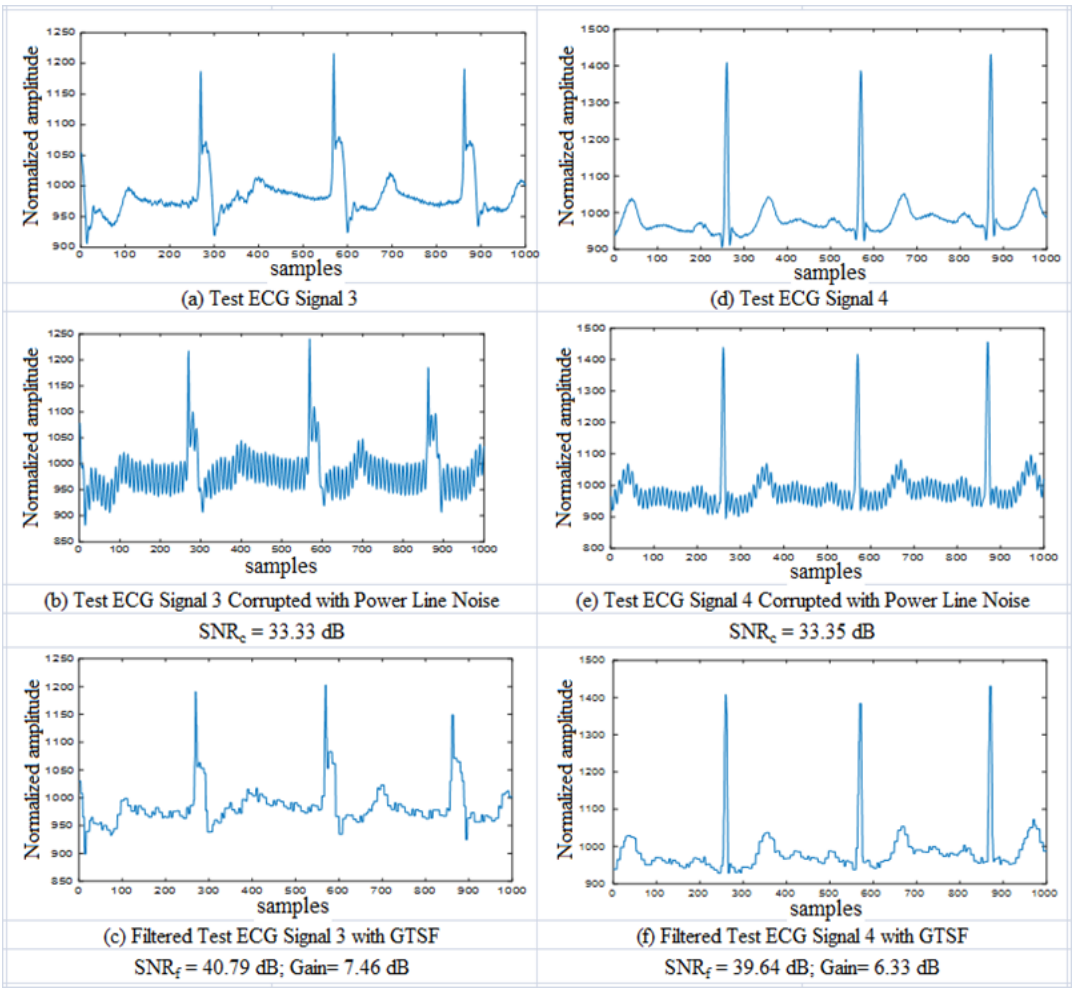

Figure 11: GTSF results for the test ECG signals 3 and 4.

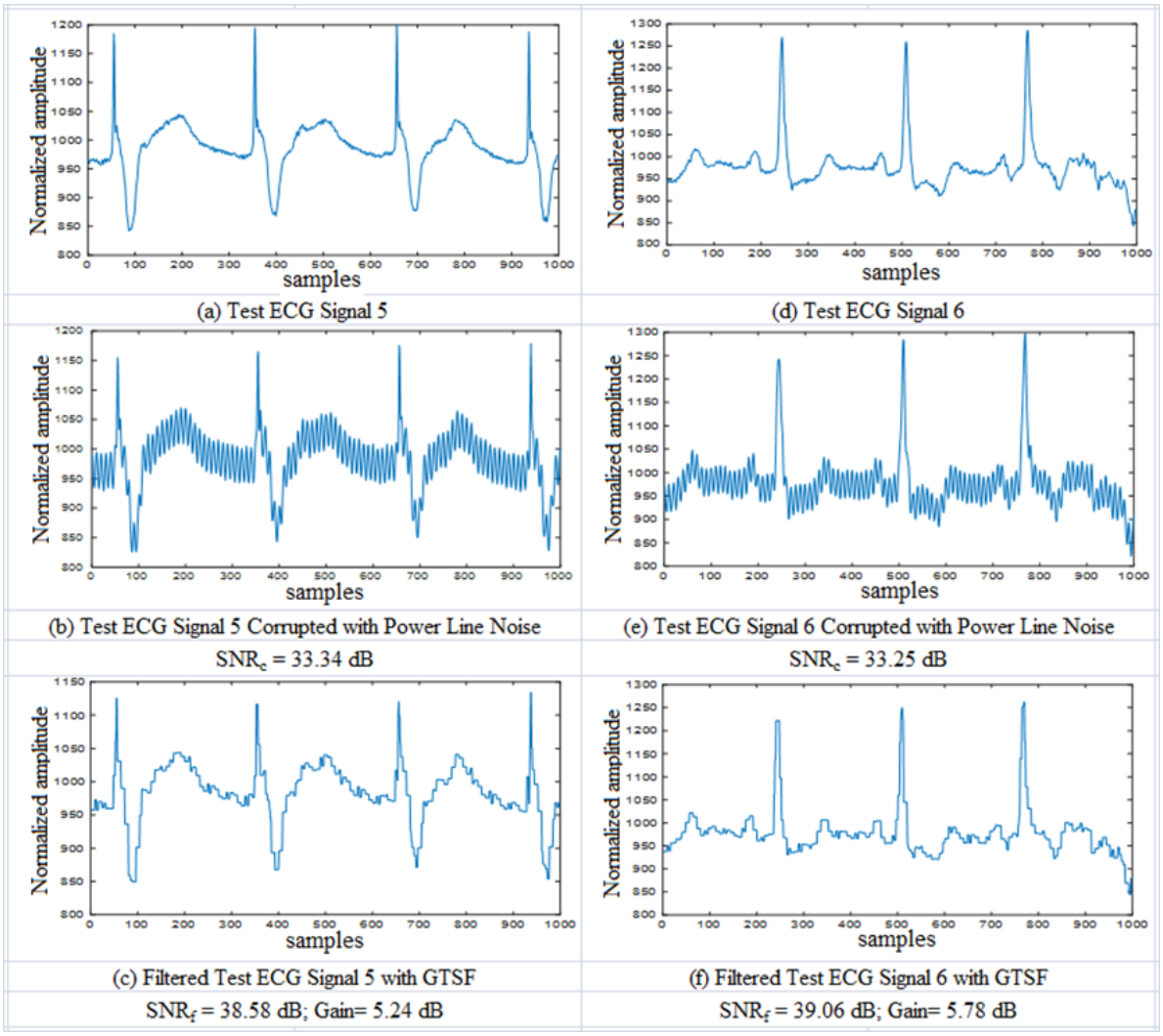

Figure 12: GTSF results for the test ECG signals 5 and 6.

The low Gain recorded for STSF in Figure 7 could be due to its constant deviation and reduction of the high coefficients which caused significant bias. Hence, it is less sensitive to small change in the data. In Figure 9, the HTSF on the other hand tends to distort the ECG signal morphology as it either shrinks or retain coefficients depending on whether it is lower or higher than the universal threshold respectively. HYTSF had moderate performance in terms of signal Gain, fairly better than STSF and HTSF as seen in Figure 7.

IV. CONCLUSION

A wavelet based PLI noise suppression algorithm has been implemented. The performance of the HTSF, STSF, HYTSF, GTSF and MGTSF for the suppression of PLI noise have been evaluated and compared. Filtering of ECG signal in the wavelet domain has been shown to be useful in the removal of PLI noise with better fidelity and higher noise suppression by testing an array of threshold shrinkage functions. Hence, diagnostic accuracy would be enhanced. In order to take this work further, other wavelet families could be employed while performance on wavelet packet tree and stationary wavelet transform (SWT) could be tested.

REFERENCES

Akwei-Sekyere, S. (2015). Powerline noise elimination in biomedical signals via blind source separation and wavelet analysis, PeerJ Life and Environment, 3(1086): 1-24. http://dx.doi.org/10.1155/2013/763903

Alfaouri, M. and K. Daqrouq. (2008). ECG signal denoising by wavelet transform thresholding, American Journal of applied sciences, 5(3): 276–281.

Aqil, M.; A. Jbari and A. Bourouhou. (2017). ECG Signal Denoising by Discrete Wavelet Transform, International Journal of Online Engineering (iJOE), 13(09): 51–68. https://doi.org/10.3991/ijoe.v13i09.7159

Aqil, M.; A. Jbari and A. Bourouhou. (2015). Evaluation of time-frequency and wavelet analysis of ECG signals, in 2015 Third World Conf. Complex Syst., 1–5.

El Bouny, L.; M. Khalil and A. Adib. (2017). Removal of 50Hz PLI from ECG signal using undecimated wavelet transform, in 2017 International Conference on Wireless Networks and Mobile Communications (WINCOM), 1–6.

El Bouny, L.; M. Khalil and A. Adib. (2019). ECG signal filtering based on CEEMDAN with hybrid interval thresholding and higher order statistics to select relevant

modes, Multimedia Tools and Applications. Springer, 78(10): 13067–13089. DOI: 10.1007/s11042-018-6143-x

El Bouny, L.; M. Khalil and A. Adib. (2017). ECG noise reduction based on stationary wavelet transform and zero-crossings interval thresholding, in 2017 Int. Conf. Electr. Inf. Technol., 1–6. DOI: 10.1109/EITech.2017.8255255

El Bouny, L.; M. Khalil and A. Adib. (2018). Performance analysis of ECG signal denoising methods in transform domain, in 2018 Int. Conf. Intell. Syst. Comput. Vis., 1–8. DOI: 10.1109/ISACV.2018.8354038

Castillo, E.; D. P.Morales; A. García; F.Martínez-Martí; L. Parrilla and A. J. Palma. (2013). Noise suppression in ECG signals through efficient one-step wavelet processing techniques, Journal of Applied Mathematics, 2013(763903): 1-13.

Chavdar, L.; M. Georgy; I. Ratcho; D. Ivan; C. Ivaylo and D. Ivan. (2005). Removal of power-line interference from the ECG: a review of the subtraction procedure, BioMedical Engineering OnLine 4(50): 1-18.

Chmelka, L. and J. Kozumplik. (2005). Wavelet-basedwiener filter for electrocardiogram signal denoising, Computers in Cardiology, Computers in Cardiology, 2005(32): 771–774.

Dandapat, S.; L. N.Sharma and R. K. Tripathy. (2015). Quantification of diagnostic information from electrocardiogram signal: A review, in Advances in communication and computing. Springer, 17–39.

Donoho, D. L. and I. M. Johnstone. (1994). Ideal denoising in an orthonormal basis chosen from a library of bases, Comptes rendus de l'Académie des sciences. Série I, Mathématique. Paris: Gauthier-Villars, c1984-c2001., 319(12): 1317–1322.

Dwivedi, A. K.; H. Ranjan; A. Menon and P. Periasamy. (2020). Noise Reduction in ECG Signal Using Combined Ensemble Empirical Mode Decomposition Method with Stationary Wavelet Transform, Circuits, Systems, and Signal Processing. Springer, 1–18. https://doi.org/10.1007/s00034-020-01498-4

Goldberger, A. L.; L. A. N. Amaral; L. Glass; J. M. Hausdorff; P. C. Ivanov; R. G. Mark and H. E. Stanley. (2000). Physiobank, physiotoolkit, and physionet:components of a new research resource for complex physiologic signals, Circulation, 101(23): e215–e220.

Goswami, J.C.; A.K. Chan. (2011). Fundamentals of wavelets: theory, algorithms, and applications, John Wiley & Sons.

Huimin, C. U. I.; Z. Ruimei and H. O. U. Yanli. (2012). Improved threshold denoising method based on wavelet transform, Physics procedia. Elsevier, 33: 1354–1359.

Kabir, M. A. and C. Shahnaz. (2012). Comparison of ECG signal denoising algorithms in EMD and wavelet domains. IJRRAS, 11(3):499–516.

Lin, Y. D. and Hu, Y. H. (2007). Power-line interference detection and suppression in ECG signal processing. IEEE Transactions on Biomedical Engineering, 55(1), 354-357.

Mateo, J.; C. Sanchez; A. Tortes; R. Cervigon; J.J. Rieta. (2008). Neural network based canceller for powerline interference in ECG signals, in 2008 Computers in Cardiology, 1073–1076.

MathWorks (MATLAB). 2019. Documentation for MathWorks products. [Online] retrieved from http://www.mathworks.com/access/helpdesk/help/helpdesk.shtml on May 1, 2019.

McSharry, P. E.; G.D. Clifford; L. Tarassenko and L.A. Smith. (2003). A dynamical model for generating synthetic electrocardiogram signals, IEEE transactions on biomedical engineering, 50(3): 289–294.

Moody,G. B. and R. G. Mark. (2001). The impact of the MIT-BIH arrhythmia database. IEEE Engineering in Medicine and Biology Magazine, 20(3): 45–50.

Opie, L. H. (2004) Heart physiology: from cell to circulation. Lippincott Williams & Wilkins.

Physiobank ATM (2018, June 10). [Online] Retrieved from https://www.physionet.org/cgi-bin/atm/ATM.

Ravandale, M. Y. V and M. S. N. Jain. (2015). Investigation of Effective De Noising Techniques for ECG Signal, International Journal on Recent and Innovation Trends in Computing and Communication, 3(4): 2261–2268.

Romero, I.; D. Geng and T. Berset. (2012). Adaptive filtering in ECG denoising: A comparative study, Computing in Cardiology, 2012(39): 45–48.

Suchetha, M.; N. Kumaravel; M. Jagannath and S.K. Jaganathan. (2017). A comparative analysis of EMD based filtering methods for 50 Hz noise cancellation in ECG signal, Informatics Med. Unlocked. 8: 54–59. http://dx.doi.org/10.1016/j.imu.2017.01.003

Tiwari, R. and R. Dubey. (2014). Analysis of different denoising techniques of ECG signals, Int. J. Emerg. Technol. Adv. Eng, 4: 2–6.

Van Fleet, P. J. (2011). Discrete wavelet transformations: An elementary approach with applications. John Wiley & Sons.,157-346.

Zubair A. R. (2019). Experiments on the capability of wavelet domain noise suppression: Comparison with spatial domain noise suppression. International Journal of Computer Applications,178(44): 53-62.

Zubair, A. R. and Ahmed, Y. K. (2019). Engineering education: Computer-aided engineering with MATLAB; discrete wavelet transform as a case study, International Journal of Computer Applications, 182(46): 6–17.

Zubair, A. R.; Y. K. Ahmed and K. A. Akande. (2018). Electromyography noise suppression in electrocardiogram signal using modified garrote threshold shrinkage function, African Journal of Computing & ICT, 11(3): 85–94.